ELSEVIER Science Press
Available online at www.sciencedirect.com
ScienceDirect
Trans. Nonferrous Met. Soc. China 30(2020) 1662−1673
Transactions of Nonferrous Metals Society of China
www.tnmsc.cn

Digestion mechanism and crystal simulation of roasted low-grade high-sulfur bauxite

Hong-fei WU[1,2], Chao-yi CHEN[1,2], Jun-qi LI[1,2], Yuan-pei LAN[1,2], Lin-zhu WANG[1,2], Bian-li QUAN[1,2], Hui-xin JIN[1,2]

1. Department of Metallurgical Engineering, College of Materials and Metallurgy,
Guizhou University, Guiyang 550025, China;
2. Guizhou Province Key Laboratory of Metallurgical Engineering and Process Energy Saving, Guiyang 550025, China

Received 14 September 2019; accepted 6 May 2020

Abstract: Low-grade high-sulfur bauxite was pretreated via suspension roasting and muffle furnace roasting to remove sulfur and enhance digestion properties. The results show that sulfur can be efficiently removed, and the alumina digestion properties are significantly improved after suspension roasting. Under optimal conditions (t=70 min, T=280 °C, w(CaO)=8% and N_k=245 g/L), the digestion ratios are 94.45% and 92.08% for the suspension-roasted and muffle-roasted ore, respectively, and the apparent activation energies are 63.26 and 64.24 kJ/mol, respectively. Two crystal models were established by Materials Studio based on the XRD patterns. The DFT simulation shows that the existing Al—O bands after suspension roasting can improve alumina digestion. The (104) and (113) planes of Al_2O_3 after suspension roasting are found to combine with NaOH more easily than those of Al_2O_3 treated in a muffle furnace.

Key words: high-sulfur bauxite; suspension roasting; reaction kinetics; digestion mechanism; crystal structure; computer simulation

1 Introduction

The rapid development of the alumina industry has resulted in an increasing demand for high-quality bauxite; however, 90% of the bauxite ores in China are diaspores. It has been reported [1,2] that nearly 14% of the diaspores in China are low-grade and high sulfur-containing bauxite (LGHS bauxite), which cannot be directly used for alumina production due to the high sulfur content. Therefore, utilizing LGHS bauxite is important to alleviate the bauxite resource shortage and contributes to the sustainable development of the alumina industry.

The sulfur in bauxite exists as SO_4^{2-}, SO_3^{2-}, S^{2-} and $S_2O_3^{2-}$ during the digestion process, which results in scarring of the digestion pipe, corrosion of equipment, and increased production cost [3,4]. The methods to remove sulfur in bauxite can be mainly divided into flotation desulfurization, bioleaching desulfurization, electrolysis desulfurization, wet oxidation desulfurization and high-temperature roasting [5]. GONG et al [5] examined the desulfurization kinetics and mineral phase evolution in a bauxite water slurry electrolysis process. LV et al [6] investigated the effects of roasting temperature, roasting time and particle size on the bauxite desulfurization performance. HU et al [7] studied the removal of sulfide by oxidative roasting and suggested that high-temperature roasting was a facile way to remove sulfide in bauxite. In addition, high-temperature bauxite roasting is beneficial for organic carbon removal and is an efficient way to

---

Foundation item: Projects (U1812402, 51774102, 51574095, 51664005) supported by the National Natural Science Foundation of China; Projects ([2015]4005, [2017]5788, [2017]5626, KY(2015)334) supported by Talents of Guizhou Science and Technology Cooperation Platform, China

Corresponding author: Chao-yi CHEN; Tel: +86-15086015817; E-mail: ccy197715@126.com

DOI: 10.1016/S1003-6326(20)65328-6

reduce the organic matter source in the Bayer process [8]. Hence, high-temperature roasting of bauxite has become a potential industrial technique for the removal of sulfur from LGHS bauxite.

High-temperature roasting will result in the evolution of the main bauxite minerals, which may affect the Al_2O_3 digestion abilities, but the mechanism of the roasting effect on the digestion of LGHS bauxite is not yet clear. On the other hand, traditional roasting processes may not be suitable for further applications [9] due to their inefficiency and over-roasting problems. Suspension roasting is an efficient roast method that has a high heat transfer and mass transfer coefficient; furthermore, suspension roasting normally requires a lower roasting temperature and a shorter roasting time than traditional roasting processes [10]. However, few investigations have focused on the influence of various roasting methods on the desulfurization ratio and Al_2O_3 digestion abilities.

Therefore, the present work aimed to reveal the influence on the desulfurization and alumina recovery of LGHS bauxite treated by suspension roasting and muffle furnace roasting. The desulfurization ratio, Al_2O_3 digestion ratio, and dynamics of alumina digestion were investigated. Moreover, the mechanism of the effect of roasting on alumina digestion was studied by DFT simulations.

2 Experimental

2.1 Materials

A LGHS bauxite sample was obtained from Guizhou Province, China, and its composition is given in Table 1. The studied LGHS bauxite has an A/S (Al_2O_3/SiO_2 ratio) of 4.07, and the sulfur content (S_T) is 2.22 wt.%. The X-ray diffraction (XRD) pattern of the bauxite is shown in Fig. 1, and the mineral composition is given in Table 2. The digestion solution used in this study was provided by an alumina factory in Guizhou, China, and its caustic soda concentration (N_k, in the form of Na_2O) was 245.05 g/L with an alumina (Al_2O_3) concentration of 134.07 g/L.

Table 1 Chemical composition of raw bauxite (wt.%)

Al_2O_3	SiO_2	Fe_T	TiO_2	S_T	LOI
52.16	12.81	11.16	3.57	2.22	18.08

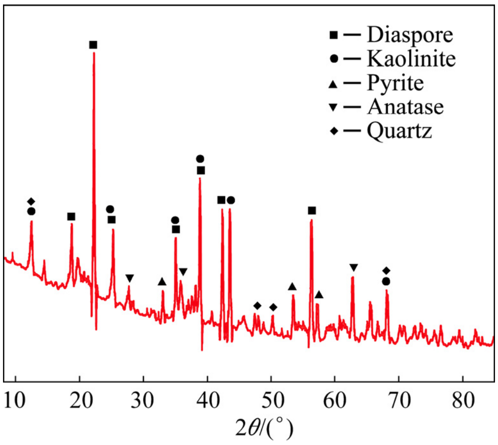

Fig. 1 XRD pattern of raw bauxite

Table 2 Mineral composition of raw bauxite (wt.%)

Diaspore	Kaolinite	Pyrite	Anatase	Quartz
56.0	27.0	9.1	3.6	4.3

2.2 Experimental methods

The raw bauxite sample was subjected to a suspension roasting system, which consisted of a gas carrier powder feeding system, a preheating route, an external circulation suspension roasting furnace, a cooling system and a powder collector. The schematic of the suspension roasting system is shown in Fig. 2. The outer diameter and length of the suspension roasting furnace were 0.4 and 9 m, respectively. After the furnace achieved a desired temperature of 600, 700, 800 or 900 °C, the bauxite powder was fed into the furnace by an air carrying gas with a feeding rate of 300 kg/h and roasted for 30, 60, 90 or 120 s. On the other hand, the same raw bauxite was roasted in a muffle furnace roasting system (MXQ 1100, China). For each roast, 30 g bauxite was placed in a ceramic boat (15 cm × 9 cm) with a layer thickness of 0.5 cm. The ceramic boat was placed in the muffle furnace with a heat rate of 10 °C/min and then roasted at the same temperature for the same time as the corresponding suspension roasting samples.

The roasted bauxite then underwent a digestion experiment in a 150 mL bomb reactor, where the reactor had a rotational speed of 10 r/min and was heated by nitrate molten salts in a furnace (±1 °C, Shandong Zhengwei Machinery Company, China). After the digestion process, the bauxite residues were filtered and washed with hot distilled water and then dried at 100 °C for 24 h.

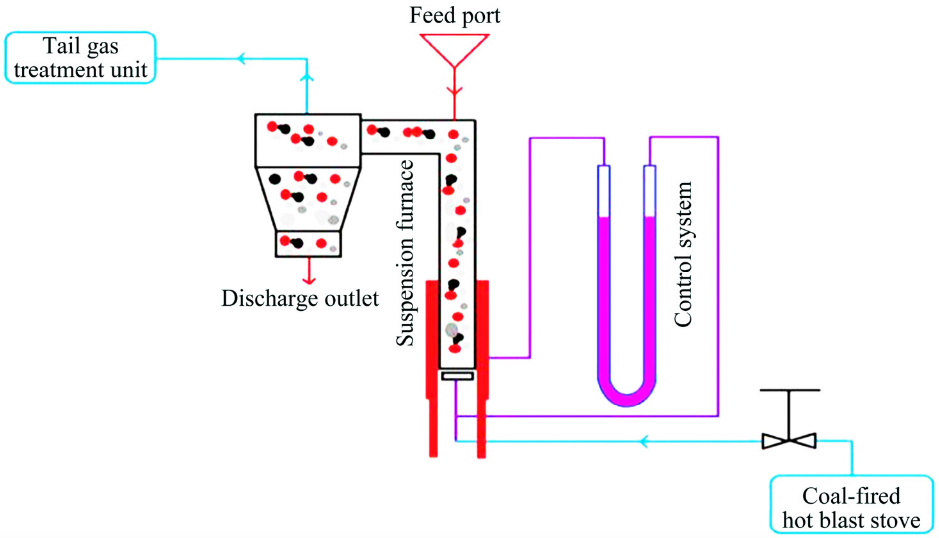

Fig. 2 Schematic diagram of suspension roasting system

The alumina digestion ratio was calculated according to

$$\eta_{Al_2O_3}=\frac{(A/S)_{ore}-(A/S)_{residue}}{(A/S)_{ore}}\times 100\% \quad (1)$$

where $(A/S)_{ore}$ and $(A/S)_{residue}$ denote the mass ratios of Al_2O_3 to SiO_2 in the bauxite ore and bauxite residue, respectively.

The batching value was calculated by

$$R_p=\frac{1.645}{R_M} \quad (2)$$

where R_M is the molecular ratio of the batching value (R_M batching value varies from 1.37 to 1.52, and in factory production, the value is normally set to be 1.40).

2.3 Analysis methods

The alumina and silica contents were analyzed by an EDTA titration method and a molybdenum blue photometric method, respectively, and the S_T in bauxite was tested by a gravimetric method. The bauxite and red mud residue samples were analyzed by XRD (Netherlands Panalytical Company) with Cu K_α radiation from 10° to 85°. HighScore Plus software (Netherlands Philips Analytical Instrument Company) was used to calculate the crystallinity and lattice parameters. To improve the accuracy of the calculation results, the main phases of the XRD patterns were first fit well, and then the integral calculation was modified with the crystallinity of 50° standard card to ensure that the value of R was less than 5%. Scanning electron microscopy (SEM) images of the ores were taken by JSM−6700F (Japanese Electronic).

2.4 DFT simulation

The calculated alumina lattice parameters according to the XRD patterns by HighScore Plus were employed as the crystal parameters to establish an Al_2O_3 crystal model by Material Studio 8.1 (Accelries Corporation, USA). Then, CASTEP was used to calculate the band structure, density of states and population analysis, under a generalized gradient approximation (GGA) functional; additionally, the *k*-point was set to be medium (1×1×1). The morphology modules were then used to calculate the surface area and surface energy based on the growth and quality of the medium.

3 Results and discussion

3.1 Roasting desulfurization

The sulfur contents of the samples that were roasted under various conditions are shown in Fig. 3. As the roasting time increased, the sulfur content decreased rapidly, which indicated that both suspension and muffle furnace roasting could remove most of the sulfur in bauxite. After the bauxite was suspension-roasted for 60 s, the S_T value was below 0.7%. Figure 3 showed that the desulfurization efficiency of suspension roasting was obviously higher than that of muffle furnace roasting for the same roasting time. Therefore, suspension roasting should be a more efficient roasting technique for removing sulfur.

3.2 Micrographs and phases of roasted bauxites

The SEM images of the roasted samples are shown in Fig. 4. The roasting method had a significant influence on the microstructure of ores. In the SEM image of the bauxite roasted in the muffle furnace, a few cracks could be found on the particle surface, while many micropores were exposed on the surface of the ore roasted by the suspension process. Cracks should be produced by the decomposition of crystalline water or the chemical reactions among different minerals after muffle furnace roasting. In the suspension roasting process, the powders were sufficiently dispersed in the gas flow, and the particle accumulation and extrusion were greatly weakened, which offered a large gas−solid contact area and high heat-mass transfer efficiency [11]. Therefore, dehydration and other reactions could be completed in a short time, and as a result, many micropores formed on the particle surface.

The XRD patterns of the bauxite roasted at different temperatures and processes are given in Fig. 5, and the calculated crystallinities are listed in Table 3. From Fig. 5, we can see that the main phases are aluminum oxide, quartz, anatase, magnetite, iron silicate and hematite. When the bauxite was roasted at 600 °C, a new mineral composition of hematite appeared in the XRD spectra of the suspension-roasted bauxite compared with the pattern of the ore roasted in the muffle furnace. Because the rate of heat and mass transfer in suspension roasting were higher than those in a muffle furnace at the same temperature, magnetite was oxidized to hematite. After the temperature exceeded 700 °C, the magnetite was completely oxidized to hematite. The main reactions occurring from 600 to 700 °C are listed as follows [9]:

$$FeS_2+O_2\rightarrow Fe_2O_3+Fe_3O_4+SO_2\uparrow \quad (3)$$

$$Fe_3O_4+O_2\rightarrow Fe_2O_3 \quad (4)$$

Furthermore, the crystallinity of the roasted ores at different temperatures is listed in Table 3. Table 3 shows that with increasing temperature, the crystallinity first increased and then decreased, and when the roasting temperature was 700 °C, the

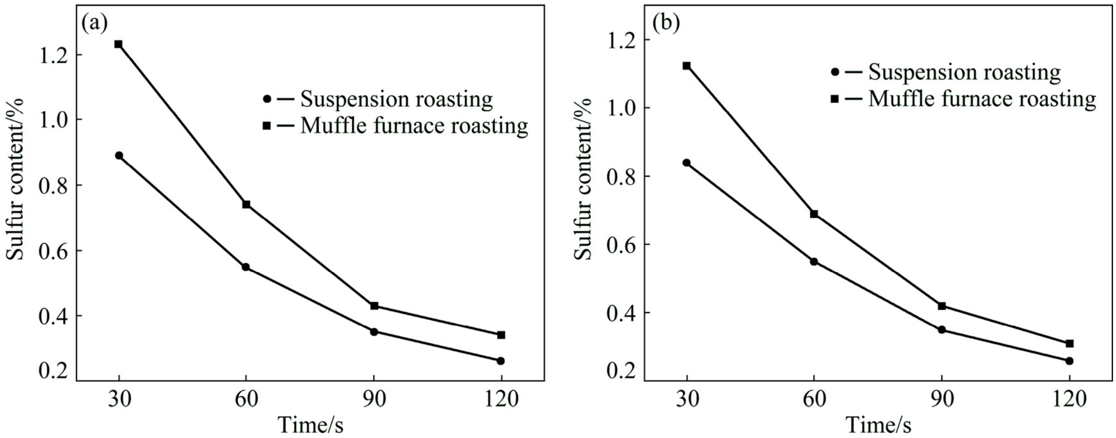

Fig. 3 Curves of sulfur content with roasting time at different roasting temperatures: (a) 500 °C; (b) 600 °C

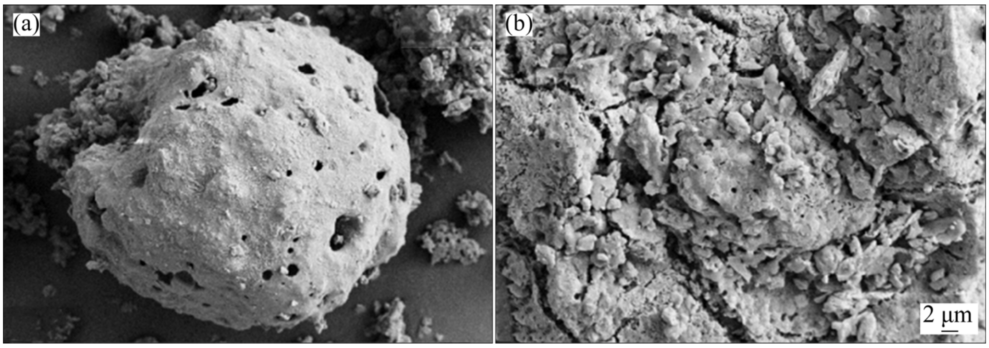

Fig. 4 SEM images of bauxite with different roasting methods at 700 °C: (a) Suspension roasting; (b) Muffle furnace roasting

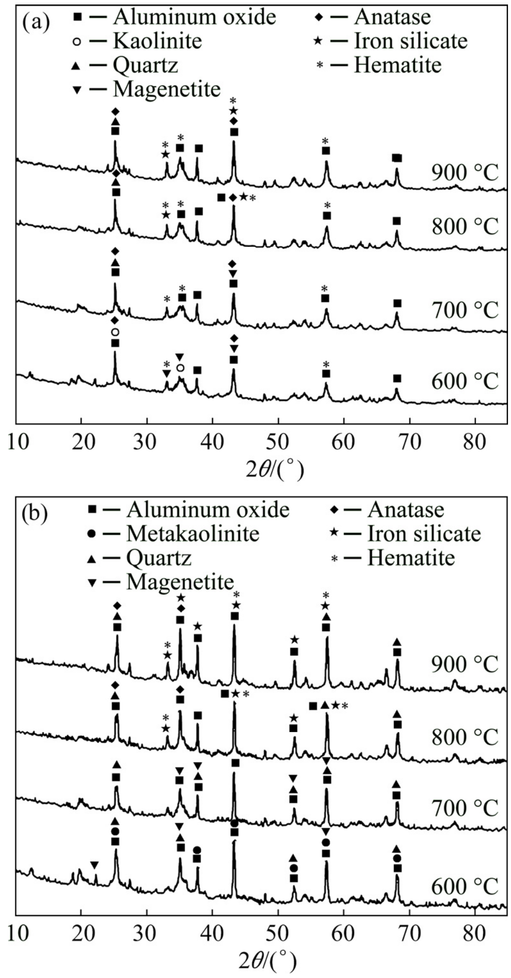

Fig. 5 XRD patterns of roasted bauxite at different roasting temperatures: (a) Suspension roasting; (b) Muffle furnace roasting

Table 3 Effect of temperature on crystallinity of roasted ore

T/°C	Crystallinity of roasted ore/%		Crystallinity of Al_2O_3 in roasted ore/%	
	Suspension	Muffle furnace	Suspension	Muffle furnace
600	14.58	11.79	7.58	7.43
700	19.94	22.14	12.76	13.06
800	19.53	19.25	12.30	12.13
900	17.21	19.20	11.53	13.25

crystallinity had the maximum value. From the calculated data, except for bauxite, which was roasted at 600 °C, the crystallinity of the minerals after being roasted in a muffle furnace was larger than that of the suspension-roasted bauxite. It was reported that metakaolinite formed in a highly disordered amorphous structure during the suspension roasting process [10]. The flash roasting and cooling process of bauxite offered a large temperature gradient that impeded the formation of regular Al_2O_3 crystals [11]. Therefore, the rapid dehydration and cooling rate during suspension roasting resulted in low crystallinity.

3.3 Al_2O_3 digestion properties

3.3.1 Effects of temperature on digestion

The effects of temperature on the digestion performance of bauxite are shown in Fig. 6. It could be seen that the temperature was positively correlated with the digestion ratio of alumina, which gradually increased with increasing temperature. The alumina digestion ratios were 95.24% and 93.06% for the suspension-roasted and muffle furnace-roasted samples at 700 °C, respectively. The digestion ratio of alumina after 700−900 °C suspension roasting was significantly higher than that of the muffle furnace roasting at the same temperature when the leaching temperature

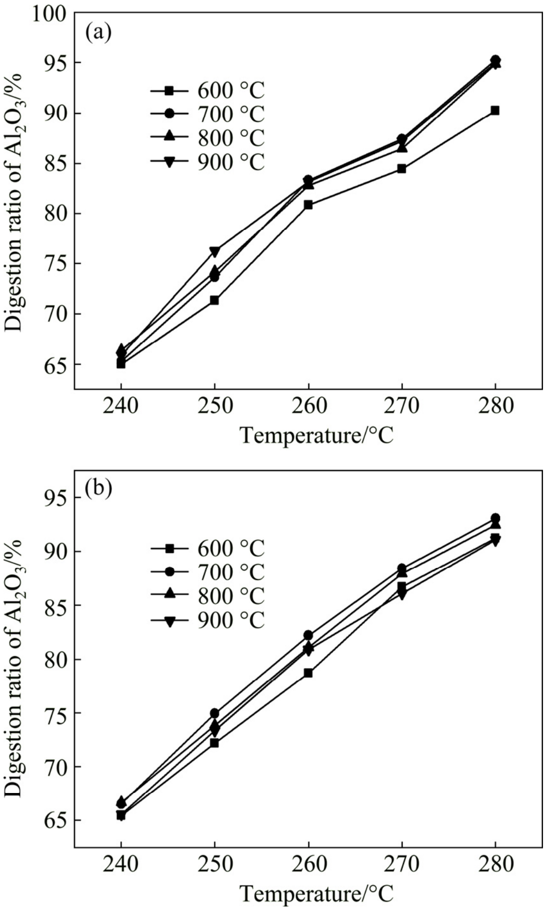

Fig. 6 Effects of temperature on digestion ratio under conditions of t=70 min, w(CaO)=8%, N_k=245 g/L and R_p=1.175: (a) Suspension roasting; (b) Muffle furnace roasting

was set to be 280 °C. The generated micropores (as shown in Fig. 4) on the particle surface increased the contact area between the ore and digestion solution, which might contribute to the elevation of the digestion properties.

3.3.2 Effects of time on digestion

Figure 7 shows the effects of time on the digestion performance of the roasted bauxite. At the same roasting temperature, the digestion ratio of alumina increased with the extension of time. The alumina digestion ratios of the bauxite roasted at 700 °C for 70 min by suspension roasting and muffle furnace roasting were 94.89% and 92.25%, respectively. Theoretically, extending the leaching time was beneficial for alumina digestion, and it was also important to convert calcium hydroxide from calcium oxide, which would promote the alumina digestion reaction [12].

3.3.3 Effects of lime addition on digestion

The effects of lime addition on the digestion performance of bauxite are shown in Fig. 8. The digestion ratio of alumina had the highest value with 8% CaO addition when the bauxite was roasted at 700 °C. In the Bayer process, adding lime could effectively improve the digestion ratio and dissolution rate, and the appropriate amount of lime could produce calcium titanate or calcium hydroxide during the digestion process to avoid the generation of a sodium titanate film and promote reaction diffusion [13,14].

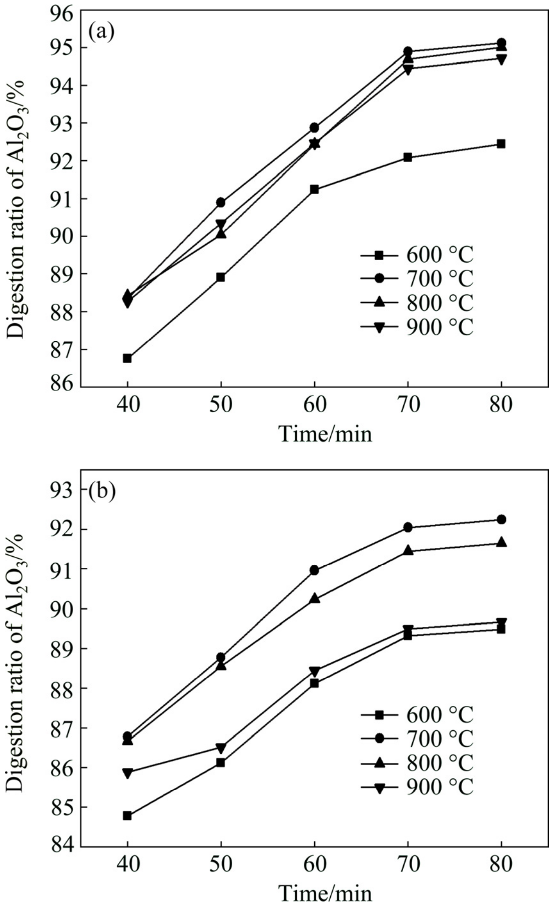

Fig. 7 Effects of time on digestion performance under conditions of T=280 °C, w(CaO)=8%, N_k=245 g/L and R_p=1.175: (a) Suspension roasting; (b) Muffle furnace roasting

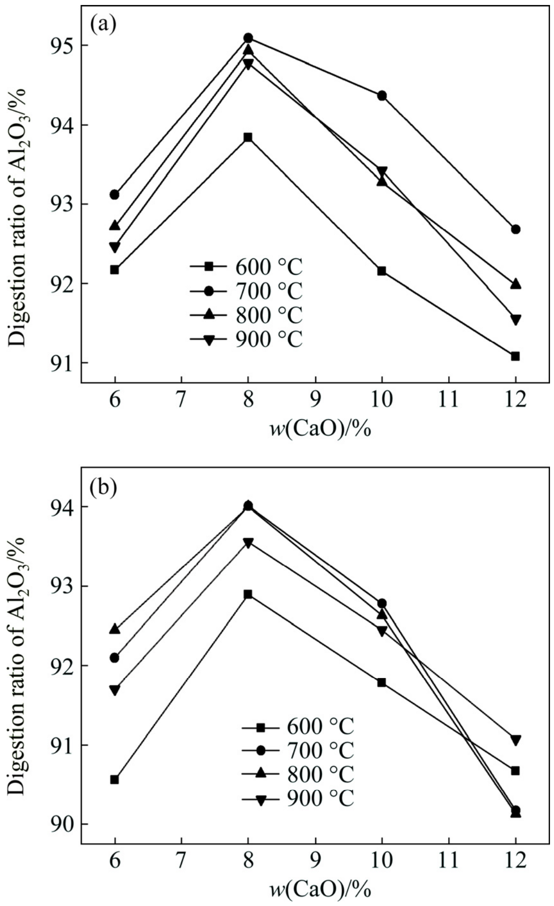

Fig. 8 Effects of lime addition on digestion ratio under conditions of T=280 °C, t=70 min, N_k=245 g/L and R_p=1.175: (a) Suspension roasting; (b) Muffle furnace roasting

3.3.4 Effects of caustic concentration on digestion

The effect of caustic concentration on the digestion performance of bauxite is shown in Fig. 9, which showed that N_k=245 g/L was the best concentration for alumina digestion. The alumina digestion ratios of the bauxite roasted at 700 °C by suspension roasting and muffle furnace roasting were 94.45% and 92.08%, respectively. A higher caustic concentration meant a higher OH^- concentration, which was beneficial to the digestion of alumina [15]. However, under certain conditions, a high caustic concentration of the digestion solution resulted in a highly viscous solution, which limited diffusion during the alumina digestion process. Therefore, the appropriate caustic concentration in this work was 245 g/L.

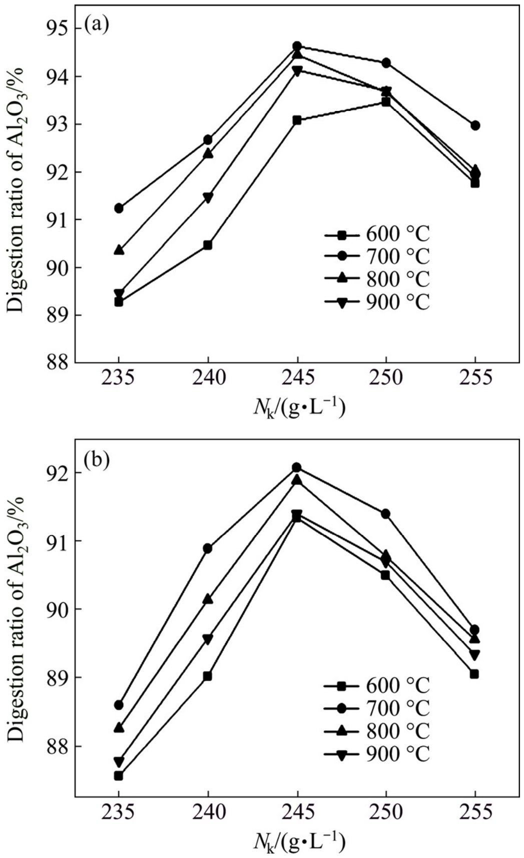

Fig. 9 Effects of caustic concentration on digestion performance under conditions of T=280 °C, t=70 min, w(CaO)=8% and R_p=1.175: (a) Suspension roasting; (b) Muffle furnace roasting

3.4 Digestion kinetics of roasted bauxite

According to the experimental data, the digestion kinetics can be simulated by related dynamics models. For the alumina digestion process, the shrinking core model is accepted as an appropriate model [16,17]. In this model, the digestion process of the diaspore is basically involved in three steps. First, the reactants diffuse toward the liquid−solid reaction surface, which is namely, external diffusion. The interface reaction is the next step, and finally, the generated products diffuse toward the solution from the interface, which is the internal diffusion [16].

Assuming that the digestion process is controlled by internal diffusion, the leaching kinetics can be simulated by the following equation:

$$1-2/3\alpha-(1-\alpha)^{2/3}=kt \quad (5)$$

where α is the digestion ratio of alumina, k is the apparent efficiency constant and t is the digestion time.

If the limiting step is a chemical reaction or external diffusion, the kinetics of the digestion process can be described by

$$1-(1-\alpha)^{1/3}=kt \quad (6)$$

To compare the effects of the two roasting methods on the digestion process, the two controlling steps mentioned above (Eqs. (5) and (6)) of the shrinking core model were investigated at different temperatures during the digestion process [17], and the results are shown in Figs. 10 and 11. According to Fig. 10, the linear relationship between $1-2/3\alpha-(1-\alpha)^{2/3}$ and t was better than that of $1-(1-\alpha)^{1/3}$ versus t. If the digestion process was controlled by internal diffusion, the internal diffusion rate of the digestion solution into the particle interior was the major factor. The internal diffusion rate increased with increasing time and digestion temperature. According to the diffusion constants at different temperatures of the digestion process, the plots of $\ln k$ versus T^{-1} were investigated, and the results are shown in Fig. 11. The correlation coefficient was above 0.97 at different temperatures. Based on the calculated results shown in Figs. 10 and 11, Eq. (5) described the kinetics better. The apparent activation energy of the digestion process based on Eq. (5) was calculated to be 64.24 and 63.26 kJ/mol for the ore after muffle furnace roasting and suspension roasting, respectively.

The two calculated apparent activation energies were similar, but the digestion ratio of alumina after suspension roasting was higher than that of muffle furnace-roasted bauxite. After suspension roasting, the newly formed α-Al_2O_3 in bauxite had a state of fine grains with high level of microstress [10]. Furthermore, the newly-formed metakaolinite existed in a disordered structure with poor crystallinity, which improved the chemical reactivity of the minerals and resulted in a high alumina digestion ratio of the suspension-roasted ore.

3.5 Analysis of roasting and digestion mechanism

To further explore enhancement mechanism of

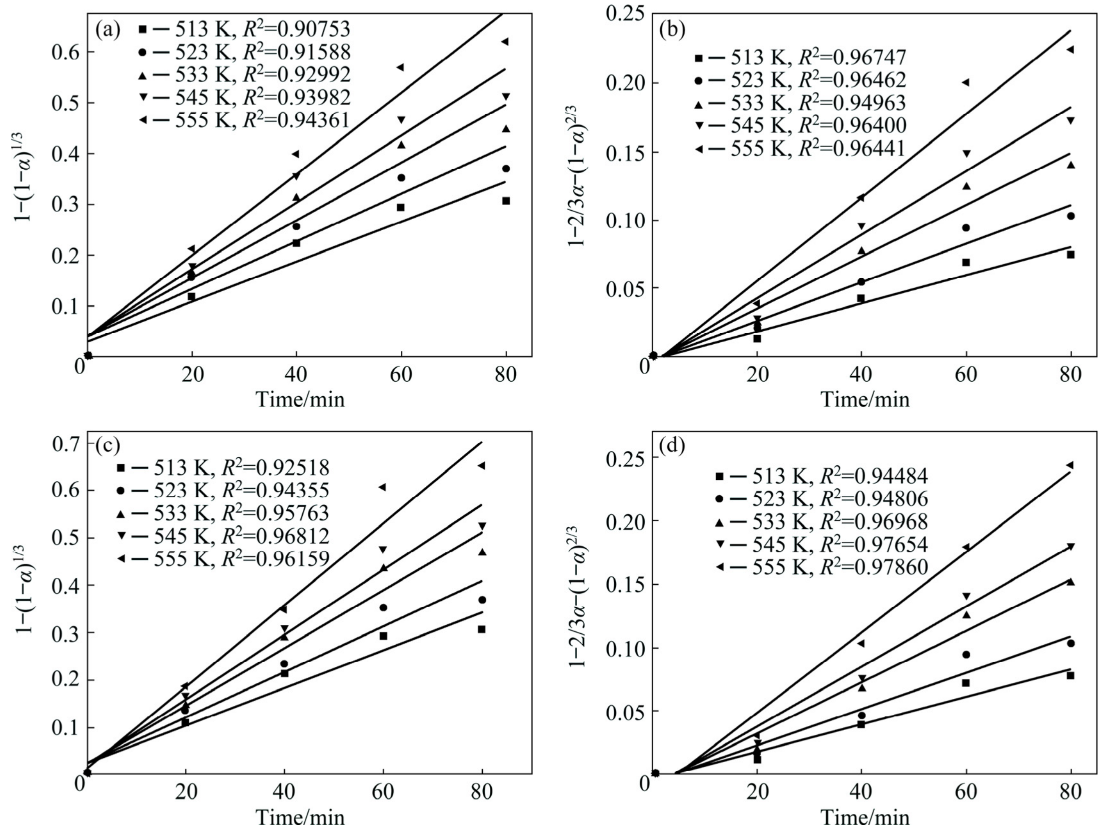

Fig. 10 Curves of digestion ratio with time for muffle furnace-roasted (a, b) and suspension-roasted (c, d) samples: (a, c) $1-(1-\alpha)^{1/3}$ vs t; (b, d) $1-2/3\alpha-(1-\alpha)^{2/3}$ vs t

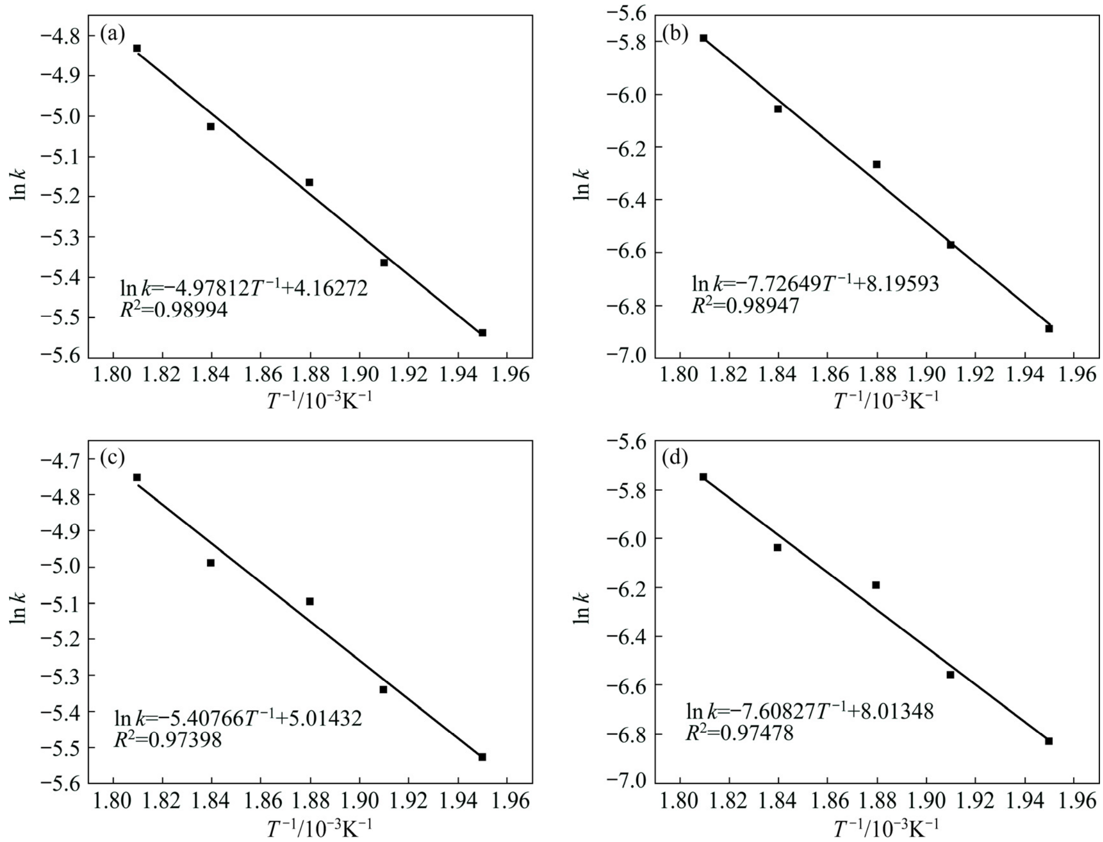

Fig. 11 Arrhenius curves of digestion for muffle furnace-roasted (a, b) and suspension-roasted (c, d) samples: (a, c) $\ln k$ vs T^{-1} for Eq. (6); (b, d) $\ln k$ vs T^{-1} for Eq. (5)

the alumina digestion ratio after suspension roasting at 700 °C, the calculated crystal parameters based on the three strong XRD peaks of the alumina phase ((104), (113) and (116)), which were obtained after refining, are given in Table 4. According to the calculated crystal parameters, two bauxite crystal models were established, as shown in Fig. 12. The CASTEP module was used to calculate the electron distribution, charge population and bond length of the two Al_2O_3 crystal models [18,19], and the results are given in Table 5 and Table 6. The binding energy between NaOH and the Al_2O_3 crystal planes was obtained and is listed in Table 7. The relationship between the crystal surface area and surface energy was calculated, and the results are shown in Fig. 13.

Table 4 shows that the lattice parameters of Al_2O_3 increase with increasing roasting temperature after suspension roasting. In addition, after muffle furnace roasting, the lattice parameters of Al_2O_3 first increase and then stabilize at 700 °C; moreover, the lattice parameters of Al_2O_3 after muffle roasting are larger than those of ores after suspension roasting. After the muffle furnace roasting, the Al_2O_3 crystal tends to be an intact phase, which makes the Al_2O_3 more difficult to dissolve. The

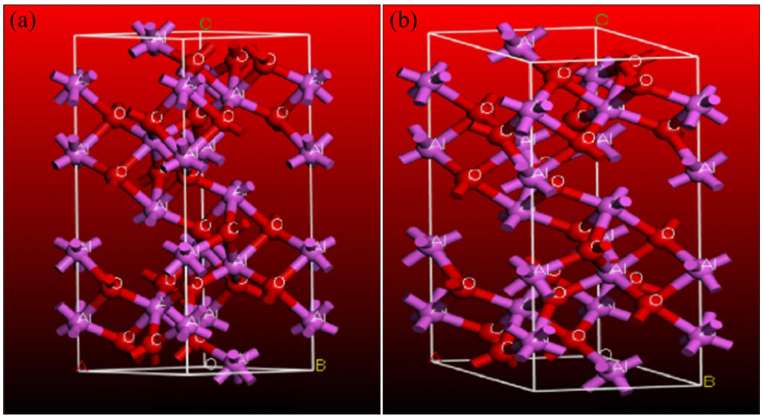

Fig. 12 Crystal structure model of Al_2O_3: (a) Suspension roasting at 700 °C; (b) Muffle furnace roasting at 700 °C

Table 4 Effect of roasting temperature on Al_2O_3 lattice parameters ($\alpha=\beta=90°$, $\gamma=120°$)

T/°C	Suspension roasting			Muffle furnace roasting		
	a/nm	b/nm	c/nm	a/nm	b/nm	c/nm
600	4.7413	4.7413	12.8919	4.7567	4.7567	12.9535
700	4.7454	4.7454	12.9026	4.7571	4.7571	13.0022
800	4.7410	4.7410	12.9254	4.7544	4.7544	12.9823
900	4.7480	4.7480	12.9185	4.7606	4.7606	13.0008
1000	4.7468	4.7468	12.9405	4.7637	4.7637	13.0007

Table 5 Al_2O_3 electron distribution of roasted ore

Suspension roasting			Muffle furnace roasting		
Bond	Population	Length/10^{-10} m	Bond	Population	Length/10^{-10} m
Al—O	0.36	1.85448	Al—O	0.36	1.85262
Al—O	0.26	1.97977	Al—O	0.26	1.96147
O—O	−0.17	2.52043	O—O	−0.17	2.52473
O—O	−0.16	2.61711	O—O	−0.16	2.61973
O—O	−0.1	2.72298	O—O	−0.1	2.72499
Al—Al	−0.49	2.65516	Al—Al	−0.49	2.65476
Al—Al	−0.63	2.78838	Al—Al	−0.63	2.79081

Table 6 Charge populations in Al_2O_3 cells

Species	s	p	Total	Charge/eV
O	1.84	5.23	7.07	−1.07
Al	0.52	0.88	1.40	1.60

Table 7 Binding energy of Al_2O_3 crystal planes with NaOH (kJ/mol)

Crystal plane	Suspension roasting	Muffle furnace roasting
(104)	12.647	13.535
(113)	14.587	16.412
(116)	19.645	18.834

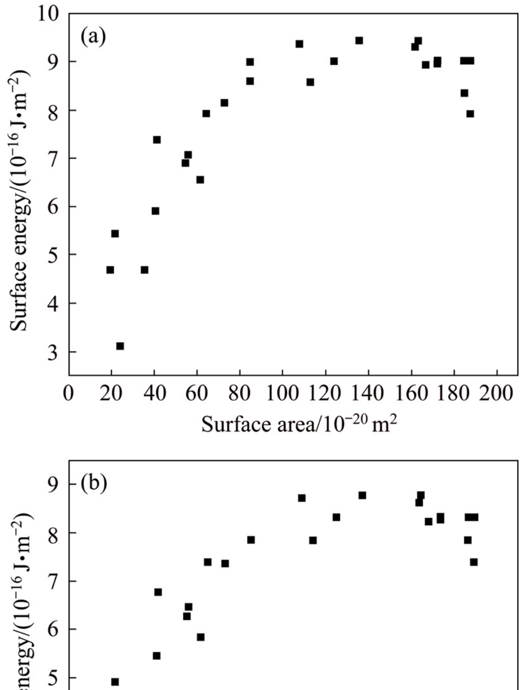

Fig. 13 Crystal surface area and surface energy of Al_2O_3: (a) Suspension roasting; (b) Muffle furnace roasting

calculated data further explain that the digestion ratio of alumina after suspension roasting is higher than that of muffle roasting under the same experimental conditions. Table 6 shows that the Al_2O_3 in the roasted ore is a typical ionic crystal [20], the positive charge of the Al is +1.60 eV, and the negative charge of the O is −1.07 eV. The Al atom is near the Fermi level and the electrons in the O 2p orbit have $2p_{\sigma-}$ and $2p_{\pi-}$ bond orbits, thus forming a strong correlation between electrons [21−23].

Table 6 shows that there are two different Al—O bonds in the Al_2O_3 crystal in roasted ore, which is due to the distortion of the $[AlO_6]$ octahedron in the corundum structure. This deformation structure reduces the crystal symmetry and changes the atomic bond length and atomic charge. The population of O—O is negative, which indicates that O—O has a strong repulsive force and that the O ions tend to move toward the octahedron in vitro [20]. From the calculation results in Table 7, we can see that the binding energies of the (104) face of Al_2O_3 to NaOH are 12.647 and 13.535 kJ/mol for the suspension-roasted and muffle furnace-roasted bauxite, respectively, which are lower than those of the (113) and (116) planes. The binding energy between Al_2O_3 and NaOH after suspension roasting is less than that of muffle furnace-roasted bauxite for the (104) and (113) planes, where the (104) plane is the predominant exposed face in the tested bauxite. During the process of alumina digestion, OH^- can not only increase the removal ratio of silica but also first penetrate into the (104) plane of Al_2O_3, cut the bonds between the crystal lattices and form free $[Al(OH)_4]^-$. Therefore, Al_2O_3 is easier to dissolve after suspension roasting process of digestion. Figure 13 shows that the surface energy of the Al_2O_3 crystal first increases and then decreases slowly. By comparing the results of the two crystal models, the surface energy of the Al_2O_3 crystal after suspension roasting is larger than that of the Al_2O_3 crystal after muffle furnace roasting. A larger surface energy promotes a strong adsorption capacity with ions in solution to achieve a stable state. Therefore, the bauxite after suspension roasting has a small apparent activation energy and easy digestion, which results in a high relative digestion ratio of alumina.

4 Conclusions

(1) Hematite started to appear in the bauxite after suspension roasting at 700 °C. The crystallinity of Al_2O_3 after suspension roasting at 700 °C was less than that of Al_2O_3 after muffle furnace roasting, which accounted for 12.76% and 13.06% of the total crystallinity of minerals, respectively.

(2) The best digestion conditions of the 700 °C roasted ore were as follows: t=70 min, T=280 °C, w(CaO)=8% and N_k=245 g/L. The digestion ratio of alumina after suspension roasting was higher than that of bauxite roasted in a muffle furnace, and the apparent activation energies were 63.26 and 64.24 kJ/mol, respectively.

(3) There were two different Al—O bonds in the Al_2O_3 crystal of the roasted ore, and the surface energy of the Al_2O_3 crystal after suspension roasting was larger than that of the Al_2O_3 crystal after muffle furnace roasting. The (104) and (113) crystal planes of Al_2O_3 after suspension roasting were easier to combine with NaOH, which might make alumina easier to dissolve.

References

[1] ZHAO Jun-cai. Quaternary karst landform and accumulative bauxite distribution rule in Western Guangxi [D]. China University of Geosciences (Beijing), 2013. (in Chinese)

[2] WANG Shi-qiang, ZHANG Zhao-hui, WANG Zhi-hui. Bryophyte communities as biomonitors of environmental factors in the Goujiang karst bauxite, southwestern China [J]. Science of the Total Environment, 2015, 538: 270−278.

[3] LI Xiao-bin, NIU Fei, LIU Gui-hua, QI Tian-gui, ZHOU Qiu-sheng, PENG Zhi-hong. Effects of iron-containing phases on transformation of sulfur-bearing ions in sodium aluminate solution [J]. Transactions of Nonferrous Metals Society of China, 2017, 27(4): 908−916.

[4] CHAI Qin-qin, YANG Chun-hua, TEO K L. Optimal control of an industrial-scale evaporation process: Sodium aluminate solution [J]. Control Engineering Practice, 2012, 20(6): 618−628.

[5] GONG Xu-zhong, ZHUANG Si-yuan, GE Lan, WANG Zhi, WANG Ming-yong. Desulfurization kinetics and mineral phase evolution of bauxite water slurry (BWS) electrolysis [J]. International Journal of Mineral Processing, 2015, 139: 17−24.

[6] LV Guo-zhi, ZHANG Ting-an, BAO Li, DOU Zhi-he, ZHAO Ai-chun, QU Hai-cui, NI Pei-yuan. Roasting pretreatment of high-sulfur bauxite and digestion performance of roasted ore [J]. Transactions of Nonferrous Metals Society of China, 2009, 19(9):1684−1689.

[7] HU Xiao-lian, CHEN Wen-mi, XIE Xiao-ling. Sulfur phase and sulfur removal in high sulfur-containing bauxite [J]. Transactions of Nonferrous Metals Society of China, 2011, 21(7): 1641−1647.

[8] CHEN Wen-mi, CHEN Xue-gang. The application of calcination oxidation on organics removal in Bayer process [J]. Light Metals, 2008(8): 10−12. (in Chinese)

[9] LV Guo-zhi, ZHANG Ting-an, ZHAO Ai-chun, BAO Li, NI Pei-yuan, LIU yan. Research on pre-roasting kinetics of high-sulfur bauxite [J]. The Chinese Journal of Process Engineering, 2010, 10(S1): s134−s137. (in Chinese)

[10] CHEN Yan-xin, ZHAO Bo, JIU Shao-wu, WU Feng, HAN Ding. Desulfurization roasting of high sulfur bauxite in suspended state [J]. Journal of Central South University (Science and Technology), 2016, 47(8): 2577−2583. (in Chinese)

[11] ZHAO Bo, CHEN Yan-Xin, JIU Shao-wu, HAN Ding, YANG Pan. Suspended roasting of high sulfur bauxite and leaching performance of roasted ore [J]. Journal of Central South University (Science and Technology), 2016, 47(9): 292−293. (in Chinese)

[12] BI Shi-wen, YU Hai-yan, YANG Yi-hong, ZHAO Fu-hui, YIN Zhong-lin, ZHAI Xiu-jing. Bayer process for the production of alumina [M]. Beijing: Metallurgical Industry Press, 2007. (in Chinese)

[13] LIU Gui-hua, LIU Yun-feng, LI Xiao-bin. Bayer leaching process reduced red mud alkali consumption [J]. Chinese Journal of Nonferrous Metals, 2006, 16(3): 555−559.

[14] PAN Xiao-lin, YU Hai-yan, TU Gan-feng, BI Shi-wen. Effect of lime on low temperature dissolution behavior of bauxite [J]. Journal of Northeastern University, 2013(4): 551−555. (in Chinese)

[15] LIU Xi-jun. Experimental study on pre-desilication of low-grade bauxite by suspension roasting and alkali leaching [D]. Xi'an University of Architecture and Technology, 2010. (in Chinese)

[16] YANG Hui-bin, PAN Xiao-lin, YU Hai-yan, TU Gan-feng. Effect of ferrite content on dissolution kinetics of gibbsitic bauxite under atmospheric pressure in NaOH solution [J]. Journal of Central South University, 2017, 24(3): 489−495.

[17] ZHU Xiao-bo, LI Wang, GUAN Xue-mao. An active dealkalization of red mud with roasting and water leaching [J]. Journal of Hazardous Materials, 2015, 286: 85−91.

[18] RUTTER M J. C_2x: A tool for visualisation and input preparation for Castep and other electronic structure codes [J]. Computer Physics Communications, 2018, 225: 174−179.

[19] TIAN Yong-pan, PAN Xiao-lin, YU Hai-yan, TU Gan-feng. Formation mechanism and crystal simulation of Na_2O-doped calcium aluminate compounds [J]. Transactions of Nonferrous Metals Society of China, 2016, 26(3): 849−858.

[20] SHANG Shun-li, WANG Yi, LIU Zi-kui. First-principles elastic constants of α-Al_2O_3 and θ-Al_2O_3 [J]. Applied Physics Letters, 2007, 90(10): 101909.

[21] FENG Jing, XIAO Bing, CHEN Jing-chao, LIANG Na. Research on band structure and DOS of sapphire by "ab-initial" methods based on DFT [J]. Journal of Kunming University of Science and Technology, 2006(4): 18−22. (in Chinese)

[22] NU Qiang, QIU Xiu-li. The electronic structure and mechanical property of alpha Al_2O_3 by first principles calculation [J]. Materials Research and Application, 2009, 3(3): 162−167. (in Chinese)

[23] WU Hong-fei, XIA Fei-long, LI Jun-qi, CHEN Chao-yi, XU Shu-tao, ZHANG Shi-heng. Digestion performance and microstructure evolution of desilicated concentrate from low-grade high sulfur bauxite [J]. Journal of Central South University (Science and Technology), 2019, 50(9): 2074−2083. (in Chinese)

低品位高硫铝土矿焙烧矿的溶出机理及晶体模拟

吴鸿飞 [1,2]，陈朝轶 [1,2]，李军旗 [1,2]，兰苑培 [1,2]，王林珠 [1,2]，权变利 [1,2]，金会心 [1,2]

1. 贵州大学 材料与冶金学院 冶金工程系，贵阳 550025；
2. 贵州省冶金工程与过程节能重点实验室，贵阳 550025

摘　要：采用悬浮焙烧与马弗炉焙烧对低品位高硫铝土矿进行预处理脱除硫和提高溶出性能。结果表明：悬浮焙烧能够有效除硫并显著提高铝土矿溶出性能，最佳溶出条件为：t=70 min，T=280 °C，w(CaO)=8%，N_k=245 g/L，悬浮焙烧和马弗炉焙烧后氧化铝溶出率分别为94.45%和92.08%，表观活化能分别为63.26和64.24 kJ/mol；基于悬浮焙烧和马弗炉焙烧铝土矿的XRD谱，通过Materials Studio建立两种Al_2O_3晶体模型。DFT模拟结果表明：相比于马弗炉焙烧，悬浮焙烧后矿物中Al—O更有利于氧化铝溶出，氧化铝晶体(104)和(113)晶面更易与NaOH结合。

关键词：高硫铝土矿；悬浮焙烧；反应动力学；溶出机理；晶体结构；计算机模拟

(Edited by Bing YANG)